

# Binary Fission and Ternary Cluster Decay of Hyper-Deformed $^{60}\text{Zn}$ at High Angular Momentum

V. Zhrebchevsky <sup>a,c</sup> W. von Oertzen <sup>a,e</sup> D. Kamanin <sup>a,b</sup>  
B. Gebauer <sup>a</sup> S. Thummerer <sup>a</sup> Ch. Schulz <sup>a</sup> G. Royer <sup>d</sup>

<sup>a</sup>*Hahn Meitner Institut-GmbH, Berlin, Germany*

<sup>b</sup>*Flerov laboratory for Nuclear Reactions, Dubna, Russia*

<sup>c</sup>*St. Petersburg University, St. Petersburg, Russia*

<sup>d</sup>*Subatech, Université-IN2P3/CNRS-Ecole des Mines, Nantes, France*

<sup>e</sup>*also Fachbereich Physik, Freie Universität Berlin, Germany*

---

## Abstract

Fission decays with two heavy fragments in coincidence have been measured from  $^{60}\text{Ni}$  compound nuclei, formed in the  $^{36}\text{Ar} + ^{24}\text{Mg}$  reaction at  $E_{\text{lab}}(^{36}\text{Ar}) = 195$  MeV (5.4 MeV/A). The experiment was performed with a unique kinematic coincidence set-up consisting of two large area position sensitive (x,y) gas detector telescopes with Bragg-ionisation chambers. Very narrow out-of-plane correlations are observed for two heavy fragments emitted in either purely binary events or in events with a missing mass consisting of 2, 3 and 4  $\alpha$ -particles. Broad distributions correspond to binary fission with the evaporation of  $\alpha$ -particles or nucleons from excited fragments. The narrow out-of-plane correlations are interpreted as ternary fission decay from compound nuclei at high angular momenta through elongated shapes with large moments of inertia, and the lighter mass in the neck region remains with very low momentum in the centre of mass frame. It is shown in calculations of shapes, that the large moments of inertia of the hyper-deformed configurations expected in these nuclei, will lower the ternary fission barrier so as to make a competition with binary fission possible.

*Key words:* HEAVY ION REACTIONS, FISSION,  $^{36}\text{Ar} + ^{24}\text{Mg}$ ,  $E_{\text{lab}} = 195$  MeV; Kinematic coincidences for heavy fragments, out of plane correlations, binary and ternary fission channels

*PACS:* 25.70.Jj, 25.70.Pq, 24.60.Dr

## 1 Introduction

Clustering and large (quadrupole) deformations are observed as general phenomena at low excitation energy in light  $N=Z$  nuclei. Rather extreme, namely hyper-deformed shapes are predicted at higher excitation energies and at high angular momenta in nuclei with masses ranging from  $A = 20$  up to 100. These hyper-deformed configurations (HD, with axis ratios 3:1) can be formed together with super-deformed (SD) configurations in heavy ion collisions. They have been discussed in various theoretical approaches [1–6]. The calculations were based mainly on the Nilsson-Strutinsky method [3–6] showing energetically favoured shapes for quadrupole deformation parameters  $\beta_2=0.6 - 1.0$  (corresponding to major-to-minor axis ratios of 2:1 up to 3:1, respectively). These shapes are stabilised due to quantal effects and represent configurations, which are several MeV lower than the liquid drop fission barriers.

Configurations corresponding to hyper-deformation are also obtained in an  $\alpha$ -cluster model [2], highlighting the relation between large deformations and clustering. For HD-states in  $N=Z$  nuclei the corresponding fission into three (or more) clusters is expected, in particular at high angular momentum. Furthermore, ternary fission is predicted using an approach based on the generalised liquid drop-model [7,8], taking into account the proximity energy and quasi-molecular shapes (as in the cluster models), i.e. for  $^{56}\text{Ni}$  and  $^{48}\text{Cr}$  nuclei. Ternary fission can be strongly enhanced for large deformations due to the larger moments of inertia creating lower fission barriers at high angular momentum and an additional lowering of the barrier by the aforementioned shell corrections. However, until now no experimental evidence for such ternary break-up of light nuclei has been reported [9–12].

We have studied fission events from the decay of the  $^{60}\text{Zn}$  compound nucleus (CN) at an excitation energy of  $E_{CN}^* = 88.0$  MeV, formed in the  $^{36}\text{Ar}+^{24}\text{Mg}$  reaction at  $E_{lab} = 195$  MeV. In the experiment two heavy fragments are measured in coincidence. Binary decays of a similar system, in the  $^{32}\text{S}+^{24}\text{Mg}$  reaction, have been studied extensively by Sanders et al. [11], and for a system of similar size ( $A=59$ ) in ref. [12], the latter, however, at a much higher energy of 8 MeV/A. From the systematic work of ref. [11] some basic information on the CN properties is available. For instance, the maximum angular momentum  $J$  reached for CN of mass  $A = 56-60$ , is close to  $J = 45\hbar$ , consistent with the predicted liquid-drop limit [10]. With the cited incident energy we reach for our system just this value of  $J$  and we expect to observe mainly the decay (including fission) from an equilibrated compound nucleus.

## 2 Experiment and results

The experiment has been performed at the ISL facility of the HMI, with the binary reaction spectrometer (BRS) [13–15]. Two detector telescopes, labelled 3 and 4, are placed symmetrically on either side of the beam axis. Each of them comprises two-dimensional position-sensitive low-pressure multi-wire chambers (MWC) and Bragg-peak ionisation chambers (BIC). In the reaction, written as  $(M_1, Z_1) + (M_2, Z_2) \rightarrow {}^{60}\text{Zn}^* \rightarrow (M_3, Z_3) + (\Delta Z) + (M_4, Z_4)$ , two heavy fragments with masses  $(M_3, M_4)$  and charges  $(Z_3, Z_4)$  are registered in kinematical coincidence and identified by their charges (and energies). The masses could not be fully determined in this experiment, however, the odd masses of the even charges are strongly suppressed relative to the even (N=Z) fragments. Details of the detectors and the experimental set-up are given in ref. [16].

With the two position sensitive detectors, correlations have been measured between two heavy ejectiles in coincidence with respect to their in-plane and out-of-plane reaction angles (see Figs. 1,2 and 3). The x- and y-read-outs give information for the angles,  $\theta$  (in plane) and  $\phi$  (out-of-plane). The two detectors cover in-plane angular ranges of  $\theta_L = 12.5^\circ - 45.5^\circ$ , and in their centre planes the out-of-plane angles  $\phi$  ranges are  $\Delta\phi = 0^\circ \pm 16.8^\circ$ , or  $180^\circ \pm 16.8^\circ$ . In contrast to previous work, the measured angular correlations represent an exclusive measurement of the binary fission yields (see for example refs. [11,12]) over a wide angular range with high resolution. Other parameters measured are the Bragg-peak height  $BP$ , the range  $R$  and the rest energy  $E$ , used for the identification of the fragments by their charge, and the momentum vectors. The reaction plane is defined by the beam axis and the vectors of the two emitted heavy fragments, coplanarity is defined by the relation  $(\phi_3 - \phi_4) = 180^\circ$ . The lighter fragments are not stopped in the BIC, but with a specific method of energy calibration of the BIC signals [17], the matched energy spectra were obtained. However, the values are not on a scale due to problems with the energy calibration.

The targets consisted of  $100 \mu\text{g}/\text{cm}^2$  of  ${}^{24}\text{Mg}$  enriched to 99.9% on a layer of  $20 \mu\text{g}/\text{cm}^2$  of  ${}^{12}\text{C}$ . Reaction channels are defined by the sum of the observed charges of the fragments registered in coincidence,  $(Z_{total} = Z_3 + Z_4)$ , with  $(Z_{total} + \Delta Z = 30)$ . The coincidences of different charges  $(Z_3 + Z_4)$  define different values of the missing charge,  $\Delta Z = 0 - 8$ . Typical two-dimensional spectra of  $BP$  versus  $R$  and  $E$  are shown in Fig. 1. For the later discussion of the potential contributions from oxygen on the target, and from the  ${}^{12}\text{C}$ -backing we will inspect the systematics of the out of plane yields (Fig. 2) and of the folding angle  $(\theta_3 + \theta_4)$  of two fragments with charges  $(Z_3, Z_4)$  in coincidence.

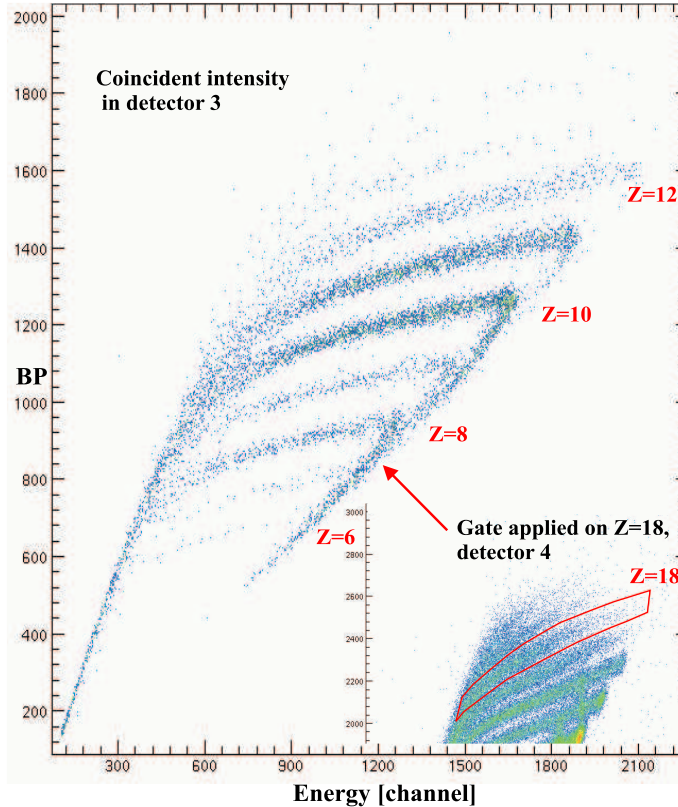


Fig. 1. Energy versus Bragg-peak (BP) distributions of events in detector 3 obtained in coincidence with a gate set for Z-identification in detector 4 (insert) for the reaction  $^{36}\text{Ar} + ^{24}\text{Mg} \rightarrow Z_3 + Z_4 + \Delta Z$ , (colour online).

For purely binary exit channels ( $\Delta Z = 0$ ), with two heavy fragments which do not evaporate charged particles, narrow out-of-plane  $\phi$ -distributions are expected. For non-binary channels broad out-of-plane distributions are observed in the  $\phi$  correlations, because of the missing information on the momenta of the unobserved third (or more) particles. A narrow distribution uniquely defines the missing momentum in the reaction plane spanned by the beam direction and the vectors of the two heavy fragments. For these events we can define coplanar ternary fission with a small momentum of the missing fragments in the centre-of-mass. These out-of-plane correlations are discussed below.

In Fig. 2 we show the total kinetic energy TKE, as a function of  $(\phi_3 - \phi_4)$ , for different combinations of  $(Z_3, Z_4)$ , and different  $\Delta Z$ . The same coincident fragment yields,  $N(Z_3, Z_4)$ , are plotted in Fig. 3 as a projection on  $(\phi_3 - \phi_4)$ . The distributions are fitted with Gaussians and the FWHM are given in the figure. For purely binary events narrow distributions around  $(\phi_3 - \phi_4) = 180^\circ$  are indeed observed, a small wider contribution results from the evaporation of neutrons. No narrow distribution is observed for  $\Delta Z = 2$ . These events are originally binary fission with an excitation energy in either fragment sufficiently high for one  $\alpha$ -particle to be emitted. The distributions become wider

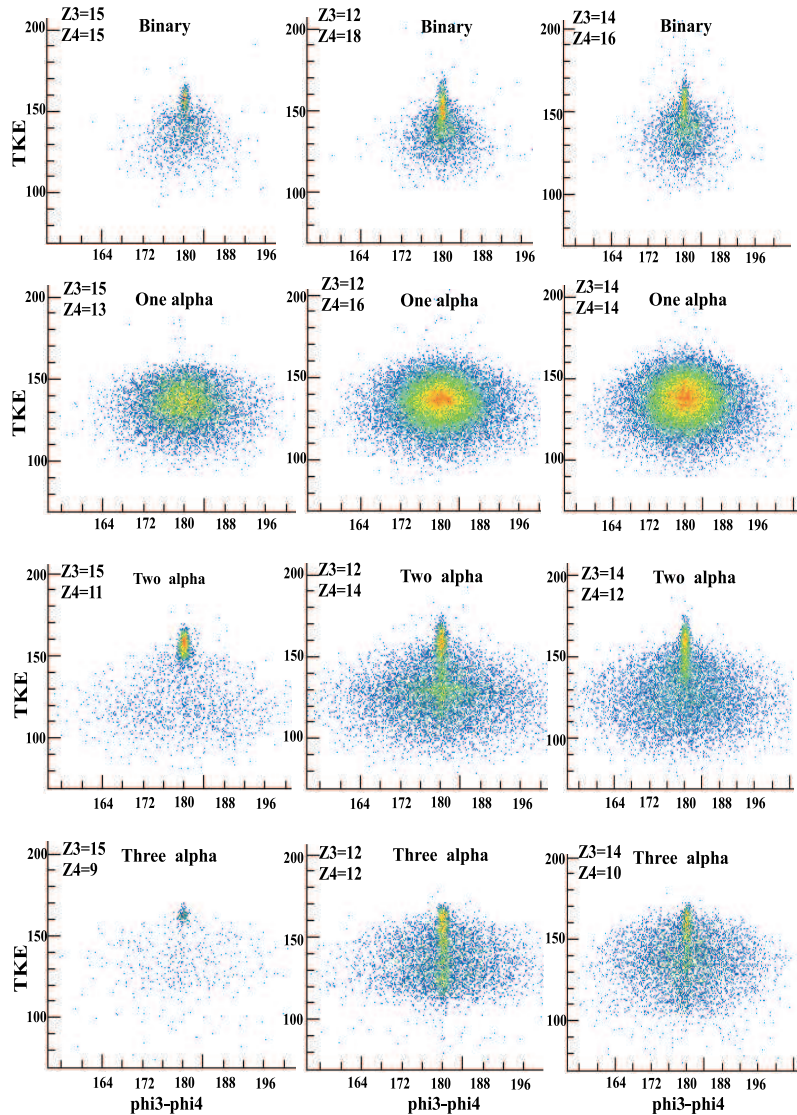


Fig. 2. Two-dimensional plots of the total kinetic energies (TKE, scale not absolute) as a function of  $(\phi_3 - \phi_4)$ , in degrees, for coincident fragments with charges  $Z_3$  and  $Z_4$ , as indicated, in the reaction  $^{36}\text{Ar} + ^{24}\text{Mg}$  at  $E_{lab} = 195$  MeV. Compare with Fig. 3. The missing number of  $\alpha$ -particles is indicated (colour online).

with increasing numbers of missing  $\alpha$ -particles, the systematics of the widths are shown in Fig. 3. We can easily identify these broad yields as fission with the excitation energy in each fragment sufficiently high to allow evaporation of 1-4  $\alpha$ -particles, respectively.

We have calculated the centre-of-mass (cm) angles,  $\theta_{cm}$ , of the different binary channels. They are approximately in the range from  $85^\circ$  to  $120^\circ$  with a variation of  $10^\circ$ , depending on  $(Z_3, Z_4)$ . The yields in the angular distributions show little variation. In this range the fission angular distributions are known to be rather flat [11,12]. We plot the fission yields (average differential cross sections) of the broad distributions for the binary fission channels in Fig. 4

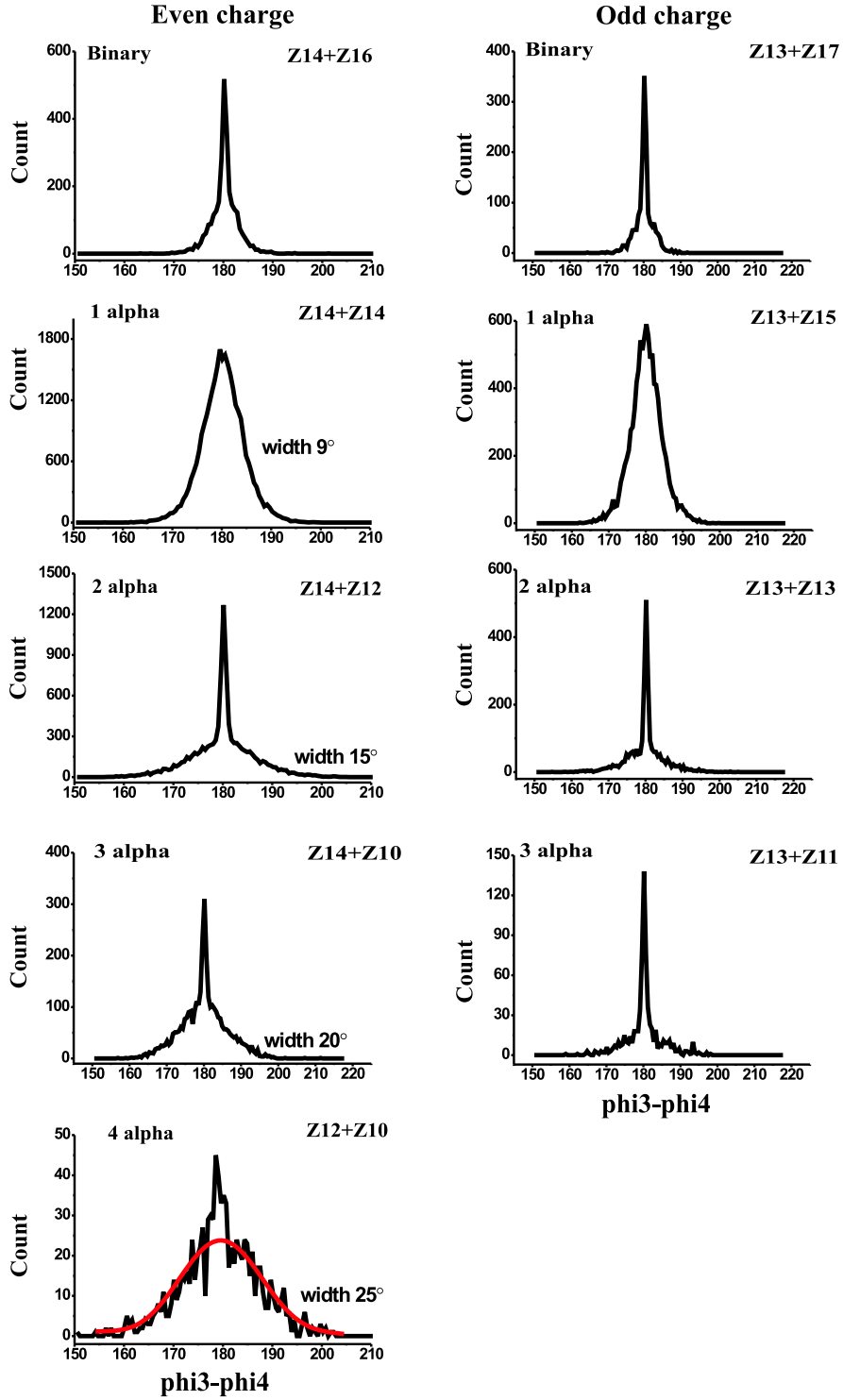


Fig. 3. Yields,  $N(Z_3, Z_4)$ , of coincident fragments with charges indicated as  $Z_3 + Z_4$ , as a function of the out-of-plane angles ( $\phi_3 - \phi_4$ ) (in degrees), for  $^{36}\text{Ar} + ^{24}\text{Mg}$  at  $E_{lab} = 195$  MeV. The widths of the angular correlations for the different channels are indicated.

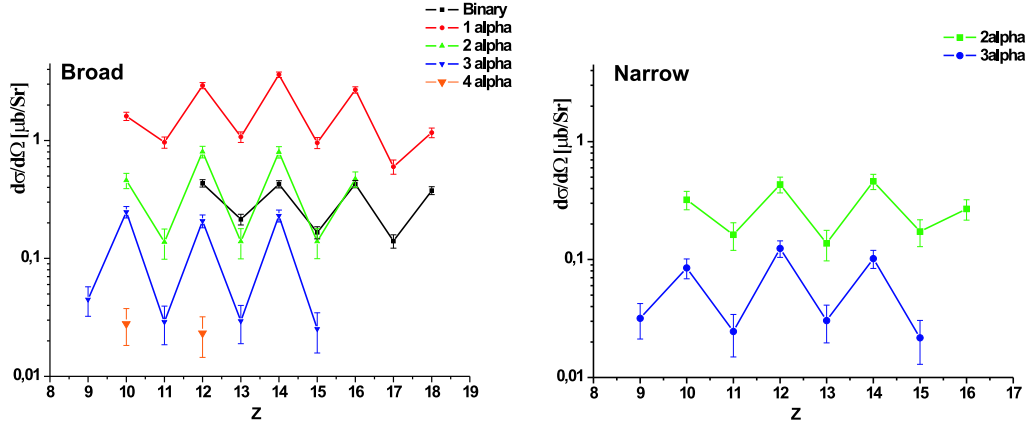


Fig. 4. Differential cross sections for channels (defined by  $Z_3+Z_4+N\alpha$ ) of the broad (binary) and narrow (ternary) components of the coincident fission fragments. They represent the average over the angular range between  $\theta_{cm}=85^\circ$  to  $115^\circ$  (statistical errors are shown). The fission channels with missing  $1\alpha$ ,  $2\alpha$ ,  $3\alpha$  and  $4\alpha$ -particles are shown.

over the cited angular range in the centre of mass. The varying ranges may introduce a systematic error of 10-20 % of the values shown in Fig. 4, the statistical errors are given with the symbols. Further systematic errors (underestimations of the cross sections) are expected for the low yields of the most negative Q-values due to the cut-off in the registration in the BIC. Also shown are the yields of the narrow components. The narrow distributions with  $\Delta Z = 4,6$  are interpreted as ternary fission, on which the following discussions below are concentrated. For the channels with large  $\Delta Z$  the ground state Q-values reach very negative values (see Tab. 1).

In the following we will discuss the origin of the narrow components. We examine if these can originate from target contaminants such as  $^{16}\text{O}$  and  $^{12}\text{C}$ .

1) We estimate the relative fission yields between reactions on  $^{16}\text{O}$  and  $^{24}\text{Mg}$ : The purely binary fission (fragments with low excitation energies and no subsequent  $\alpha$ -decay) from the compound nucleus  $^{60}\text{Zn}$  has a small yield. The cross sections for the emission of excited fragments with corresponding additional emission of  $1\alpha$ - and  $2\alpha$ -particles are the largest. The fission yields leading to the corresponding broad distributions are typically five to ten times larger than the purely binary channels. This fact gives us the possibility to estimate the contribution from the target contaminants. If the narrow component for  $\Delta Z = 4$  originates from a binary fission process of  $^{52}\text{Fe}$  (from a  $^{16}\text{O}$  target), we expect a corresponding dominant contribution for  $-1\alpha$ -decay in the  $\Delta Z = 6$  distributions. We find that the experimental yield in the wide  $\Delta Z = 6$  distributions is a factor 10 to small to originate from  $^{16}\text{O}$ , as illustrated in Fig. 5. In this figure the binary  $-1\alpha$ -yields related to the respective purely binary yields (narrow parts) are indicated: first for  $^{60}\text{Zn}$ , then for  $^{52}\text{Fe}$ , and

the last for  $^{48}\text{Cr}$ , respectively. The result shows that the contributions from  $^{16}\text{O}$  would be in the range of 10%.

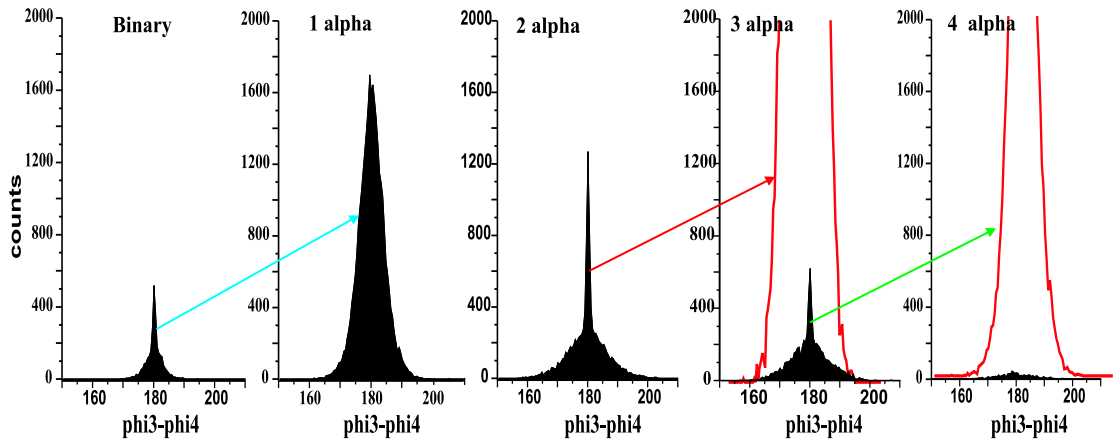


Fig. 5. Out-of-plane distributions with indications of the  $-1\alpha$  yields of the respective narrow components for the determination of contributions from contaminants in the target (see text for more details).

2) Similar considerations apply for the  $^{12}\text{C}$  in the target, it will be manifested in the narrow component in the yield for  $\Delta Z = 6$ . If all events in this narrow component would originate from a binary process on  $^{12}\text{C}$ , a corresponding strong wide component must appear in  $\Delta Z = 8$ .

3) The width of the broad out-of-plane distribution gives another important indication. The expectation is that for larger charge losses  $\Delta Z > 2$  (a statistical emission of several charged particles from the fragments) the  $(\phi_3, \phi_4)$ -correlations have increasing width. This is indeed fulfilled (see Fig. 3) for the broader component. For  $\Delta Z=4$ ,  $\Delta Z=6$ , and  $\Delta Z=8$  in Figs. 2 and 3, the width increases continuously from  $9^\circ$  for  $(-1\alpha)$ ,  $15^\circ$ ,  $21^\circ$  and  $25^\circ$ , respectively, up to the yields for  $-4\alpha$ . This would not be the case if an appreciable amount of these yields would originate from  $^{16}\text{O}$ .

4) We have estimated the target thickness for  $^{16}\text{O}$  needed if the narrow component in  $\Delta Z=4$  is completely due to the binary fissions of  $^{52}\text{Fe}$  (with the same cm cross section as for  $^{60}\text{Zn}$ ) and find that three times more  $^{16}\text{O}$  is needed than is possible for a completely oxidised target. Assuming a (rather large) 30% contamination due to oxidation again a missing factor of 10 is found.

5) The folding angles in  $\theta_3 + \theta_4$  of the two fragments can be used to distinguish two different reactions. However, due to the very negative Q-values of the reactions on  $^{24}\text{Mg}$ , the corresponding kinematics of the reactions on  $^{16}\text{O}$  (with the emission of two  $\alpha$ -particles) overlap completely with the former in the  $\theta$ -correlations for the registered angular range. Thus, no separation is possible.

6) The higher kinetic energy of the narrow component. As discussed below the

third (ternary) fragments are assumed to be created in the neck, and will have rather low kinetic energy in the cm system. We have performed calculations of the corresponding collinear three-body decay. These cases imply for example that the missing particle  $X$ , a  ${}^8\text{Be}$  nucleus (or  ${}^{12}\text{C}$ ) is emitted “backwards” from one of the moving heavier fragments with a corresponding momentum  $P_3 = -P_X$  to obtain a negligible value of its momentum in the cm, and this gives us the upper limit of the TKE. The resulting values of the TKE are approximately 20-30 MeV higher than the centre of the broad component in the energy distributions. These observations show that the narrow yields must originate dominantly from fission of  ${}^{60}\text{Zn}$  ( ${}^{24}\text{Mg}$  target). Our estimate is that  $\approx 10\%$  of the narrow distributions  $\Delta Z = 4, 6$  originate from target contaminants.

### 3 Discussion of binary and ternary fission

For the discussion of the fission process the systematics of the differential cross sections shown in Fig. 4 are inspected further. We find in these data an odd-even effect of the fission yields, with the suppression of the odd charges. The following discussion will show, that this is clearly due to the less favourable Q-values for the odd-odd fragments (see Tab.1). The fission process in the standard statistical decay theory is governed by the Q-values and the level densities at the saddle point. The “enhancement” for odd-odd charges predicted in the work of Gupta et. al. [21], where no phase space is used, is in clear contradiction with the present result. As a final statement concerning these systematics, we note the very low yield of the combinations with  $\Delta Z = 8$ , due to their very negative Q-values.

We will show that the competition between binary and ternary decays is only possible at the highest angular momenta. The narrow component observed in the  $(\phi)$ -correlations at  $(\phi_3 - \phi_4) = 180^\circ$  implies a particular geometrical three-body configuration. Three fragments could be placed at different relative orientations, however, it can easily be shown that for larger values of the total spin  $J$ , the *collinear configuration*, which has the largest moment of inertia relative to all others, gives the lowest fission barrier. This feature has been calculated for some specific cases by Wiebecke and Zhukov [20].

The experimental results also indicate that the missing particles are dominantly multiples of  $\alpha$ -clusters. Such behaviour is predicted by the  $\alpha$ -cluster model (see third diagram of Fig. 3 in ref. [2] for the hyper-deformed  ${}^{56}\text{Ni}$ ). The breaking of an  $\alpha$ -particle to produce odd (or odd-odd) fragments implies configurations, which are structurally and energetically strongly unfavoured.

For the interpretation of the reaction mechanisms, which can give the narrow components in the  $\phi$ -correlations, we shortly consider three different processes.

- i) Pre-fission emission: a fission process after emission of nucleons, or of one or two  $\alpha$ -particles. Such a pre-scission process would not disturb the out-of-plane correlation of the two remaining fission fragments. We can rule out this process by the following arguments. Following the systematics of Morgenstern [18], the average energy carried away in compound decay by one nucleon is 16.4 MeV, and by one  $\alpha$ -particle it is 23.4 MeV, and the prefission values would be even higher. For such a CN with reduced excitation energy, it is known that no second chance fission can be expected [11,19]. No significant contribution from a narrow peak in the  $(\phi_3, \phi_4)$ -correlations is observed for the fragment-fragment coincidences with one missing particle, for  $\Delta Z=1$  or 2.
- ii) A binary fission process with strong spin alignment in the fragments, e.g. for  $\Delta Z=4$ . Two  $\alpha$ -particles must be evaporated correlated in-plane from two primarily excited heavy ejectiles with their angular momenta completely aligned perpendicular to the reaction plane. The alignment from the first step would have to be preserved for the whole set of data  $\Delta Z=2-6$ , in order to produce the narrow distributions.
- iii) Ternary fission as discussed before. This can be a prompt ternary decay, in the collinear geometry. More likely the ternary fragments are emitted in a sequence of two fast fission processes with two neck ruptures in short time sequence, shorter than the average fission time. As we will show below, the energy balance allows the ternary processes to occur only for the highest angular momenta emphasising the cited geometry.

#### 4 Statistical model for binary and ternary fission

A major point in the interpretation of the data is to explain the relative yield of the “ternary” to the binary fission channels in view of their Q-values. We have to consider the statistical phase space and the saddle points for both binary and coplanar ternary fission. This can be achieved by using the formalism of the Extended Hauser-Feshbach Method (EHFM) [19]. For ternary events, implying  $N\alpha$ -particles in the neck, we can assume that these remain with very low momentum in the centre of mass. Therefore, we will neglect the phase space of these particles (in cm), as well as their kinetic energy. For a CN with excitation energy,  $E_{CN}^*$ , a Q-value  $Q_{gs}(3,4)$ , an excitation energies of the fragments given by  $U_3$ ,  $U_4$ , and their relative kinetic energy as  $E_{kin}(3,4)$ , we have the constraint:  $U_3 + U_4 = E_{CN}^* + Q_{gs}(3,4) - E_{kin}(3,4)$ . The two excitation energies are connected via energy conservation and both fragments being registered in coincidence before further decay, their excitation energies,  $U_3$  and  $U_4$ , are below the  $\alpha$ -decay threshold. For even-even nuclei with (N=Z) this is in the region of 5-9 MeV, and the Coulomb barrier of the  $\alpha$ -particles must be added.

Defining the total spin  $J$ , of the CN, and a distance parameter  $r$  between the

two fragments, which stands for the shape of the fission saddle, we can discuss the total energy balance. We define the free energy, which will determine the yield for a particular partition, with the potential energy for the relative motion of fragments 3 and 4 as  $V_{pot}^{eff}(J, 3, 4, r)$ :

$$E_{free}(3, 4, J) = E_{CN}^* + Q(3, 4) + V_{pot}^{eff}(J, 3, 4, r), \quad (1)$$

For negative Q-values and large  $J$ , the values of  $E_{free}(3, 4, J)$  and the yields tend to zero. The rotational energy  $E_{rot}(J, 3, 4, r)$  in  $V_{pot}^{eff}(J, 3, 4, r)$  depends on the total spin  $J$  and on the moments of inertia  $\Theta_{ff}(r)$ . The total potential will also contain the shell corrections  $\Delta_{sh}(r)$  at the deformed saddle point:  $V_{pot}^{eff}(J, 3, 4, r) = E_{rot}(J, 3, 4, r) + V_{pot}(3, 4, r) + \Delta_{sh}(r)$ . The values of the shell corrections for hyper-deformed shapes are in the range of 5-8 MeV for  $N=Z=28$ , see the review by Ragnarson et al. [6]. Within the statistical

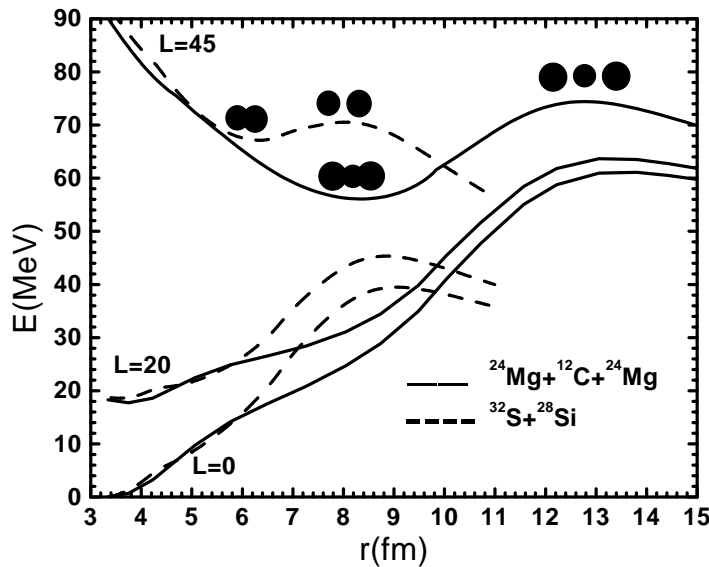


Fig. 6. Potential energies (in MeV) obtained in the liquid-drop model for selected fragmentations in the decay of  $^{60}\text{Zn}$  as a function of the deformation (represented by the distance  $r$  between the two heavier fragments) for different angular momenta (in units of  $\hbar$ ) for binary and ternary fission, respectively.

model the relative yields of the binary and ternary fission can be obtained. They will depend: a) on the different Q-values (see Tab. 1), and thus finally on the different values of  $E_{free}(3, 4, J)$ . This will result in different values of

$U_i$ ; b) on the moments of inertia  $\Theta_{ff}$  entering into  $V_{pot}^{eff}(J, 3, 4, r)$ , and the corresponding fission barrier heights, some relevant values are summarised in Tab. 1; c) on the shell corrections to  $V_{pot}^{eff}(J, 3, 4, r)$  for large deformations (3:1 axis ratio) lowering the fission barriers.

Due to the increase with angular momentum of  $V_{pot}^{eff}(J, 3, 4, r)$ , the free energy  $E_{free}(3, 4, J)$  at the saddle point is dramatically reduced with increasing  $J$ , with a lower increase of the former for the ternary decay. Given the large difference in Q-value shown in Fig. 6 and Tab. 1, the barriers for binary and ternary fission become comparable only at the highest angular momenta of the compound nucleus. The more negative Q-value for ternary fission is compensated by the smaller value of  $E_{rot}(J, 3, 4, r)$  at the saddle point, which occurs at larger distances for ternary fission. In Tab. 1 the Q-values are shown and in Fig. 6 the rotational energies at the saddle point for  $J = 45\hbar$ , which determine the penetrabilities for the heavy fragments. For negative Q-values negligible contributions are expected at low angular momentum. For the case of ternary fission with  $\Delta Z=8$  the barriers are so high that only very small yields of ternary fission become possible.

Table 1

Barrier heights in MeV for fission channels of  $^{60}\text{Zn}$  for two values of  $J$ , the angular momentum in the CN and Q-values with the fragments in their ground states.

Reaction	$Barrier(J = 0)$	$Barrier(J = 45)$	Q-value [MeV]
<i>Binary</i> , $-0\alpha$ , $^{32}\text{S} + ^{28}\text{Si}$	39.5	70.5	+ 3.34
<i>Binary</i> , $-0\alpha$ , $^{30}\text{P} + ^{30}\text{P}$	46.7	77.6	- 3.76
<i>Binary</i> , $-1\alpha$ , $^{28}\text{Si} + ^{28}\text{Si}$	40.9	55.2	- 6.64
<i>Ternary</i> , $-2\alpha$ , $^{26}\text{Al} + ^{26}\text{Al}$	66.2	79.4	- 24.59
<i>Ternary</i> , $-2\alpha$ , $^{28}\text{Si} + ^{24}\text{Mg}$	55.3	68.5	- 13.58
<i>Ternary</i> , $-3\alpha$ , $^{24}\text{Mg} + ^{24}\text{Mg}$	61.2	74.4	- 23.57

The Q-values with odd-odd charge fragments for binary and ternary mass splits are in addition 5-10 MeV more negative, this fact is the origin of the reduced cross sections for odd-odd fragments (Fig. 4) in both, binary and ternary fission channels. In these cases lower yields and fewer subsequent decays via particle evaporation are possible. The narrow peaks in the  $(\phi_3, \phi_4)$ -correlations dominate the spectra if the sum of two odd charges is taken (Fig. 2).

The yields shown in Fig. 4 confirm the statistical-model predictions, *i.e.* the specific dependence of the yields on the Q-values; the odd-even effect in the yields is clearly observed. The odd-odd yields are a factor 5-10 smaller than the corresponding yields for even-even fragments. The yields of the ternary decay are smaller for the same  $\Delta Z$ -values, due to their more negative Q-values, and a similar odd-even effect is observed. We expect that the lowering of the ternary

fission barrier due to shell corrections supports the observation of ternary fission.

## 5 Conclusions

We conclude that the observation of the narrow coplanar fission-fragment in the exclusive coincidences in the present work is a unique feature, which can only be observed with the described (or similar) experimental set-up. It gives evidence for the occurrence of a ternary decay process. Although a more detailed analysis within the statistical model still needs to be done, the relative yields in the different channels clearly show features of a statistical decay at equilibrium. The odd-even staggering in the yields of binary and ternary fission processes as a function of charge, appears as expected, with the lower yields for the odd charges with more negative Q-values. This is in total disagreement with the recently published work of ref.[21], where without the use of the statistical model and the corresponding phase space a high yield for the odd-odd fragments was predicted for the binary fission of  $^{56}\text{Ni}$ .

Remarkable, is the preference for decays where the third fragment appears as multiple of  $\alpha$ -particles (2 or 3). This indicates that the hyper-deformed nucleus in its structure is highly clustered, as actually predicted in the Brink-Bloch cranked  $\alpha$ -cluster model [2]. The neck represents a region of low nuclear density favouring the formation of  $\alpha$ -clusters, as discussed by Horiuchi [22].

The present work also shows that the search for hyper-deformation in rapidly rotating nuclei can be pursued with charged-particle spectroscopy. For nuclei in the medium-mass region with  $N=Z$  a complete reconstruction of the ternary fission events could be undertaken with additional appropriate detectors. Thus, measurements of the ternary fission process will offer the possibility for detailed spectroscopy of extremely deformed nuclear states.

We thank H.G. Bohlen, C. Wheldon and Tz. Kokalova for their numerous discussions on this project. V. Zherebchevsky thanks the DAAD for a grant.

## References

- [1] S. Cohen, F. Plasil and W. J. Swiatecki, *Ann. Phys. (N.Y.)* **82** (1974) 557.
- [2] J. Zhang, A. C. Merchant, and W. D. M. Rae, *Phys. Rev. C* **49** (1994) 562 and W.D.M. Rae in *Proc., 5<sup>th</sup> Intern. Conf. on Clustering Aspects in Nuclear and Subnuclear Systems 1988*, Kyoto, *Prog. Theor. Phys. (Jap.)* ed. K. Ikeda, (1989) p. 80.

- [3] G. Leander and S. E. Larsson, Nucl. Phys. **A 239** (1975) 93.
- [4] S. Aberg, H. Flocard and W. Nazarewicz, Ann. Rev. Nucl. Science, Vol. **40** (1990) 439.
- [5] S. Aberg and L. O. Joensson, Z. Phys. **A 349** (1994) 205.
- [6] I. Ragnarsson, S. Aberg and R.K. Sheline, Phys. Scr. **24**, 215 (1981); I. Ragnarsson, S.G. Nilsson and R.K.Sheline, Phys. Rep. **45** (1978) 1.
- [7] G. Royer and F. Haddad, J. Phys. **G 21** (1995) 339.
- [8] G. Royer, J. Phys. **G 21** (1995) 249; also G. Royer, F. Haddad and J. Mignen, J. Phys. **G 18** (1992) 2015.
- [9] N. Curtis et al. , Phys. Rev. **C 53** (1996) 1963.
- [10] C. Beck and A. Szanto de Toledo, Phys. Rev. **C 53** (1996) 1989.
- [11] S. J. Sanders, A. Szanto de Toledo and C. Beck, Phys. Rep. **311** (1999) 487 and references therein.
- [12] Sl. Cavallaro et al., Phys. Rev. **C 57** (1998) 731 and references therein.
- [13] B. Gebauer et al., in Proc. Int. Conf. on the Future of Nucl. Spectroscopy, Crete, Greece, 1993, eds. W. Gelletly et al., p. 168.
- [14] B. Gebauer et al., 2003, *Achievements with the Euroball spectrometer*, eds. W. Korten and S. Lunardi, p. 135.
- [15] C. Beck et al., Nucl. Phys. **A 734** (2004) 453.
- [16] S. Thummerer et al., Nuovo Cimento **111 A** (1998) 1077, and Ph.D. Thesis, 1999, Freie Universität Berlin.
- [17] V. Zhrebchevsky, (2006), Ph.D. Thesis, St.Petersburg University, to be published
- [18] H. Morgenstern et al., Z. Phys. **A 313** (1983) 39.
- [19] T. Matsuse, C. Beck, R. Nouicer and D. Mahboub, Phys. Rev. **C 55** (1997) 1380.
- [20] H. J. Wiebecke and M. Zhukov, Nucl. Phys. **A 351** (1981) 321.
- [21] R. J. Gupta, C. Beck, and W. Greiner, Phys. Rev. **C 71** (2005) 014601
- [22] H. Horiuchi, Nucl. Phys. **A 731** (2004) 329.